21st Australasian Fluid Mechanics Conference
Adelaide, Australia
10-13 December 2018

# Simulation of Forced Ignition in a Mach 6 Scramjet Combustor

**D. R. Curran[1], V. Wheatley[1] and M. K. Smart[1]**

[1]Centre for Hypersonics
The University of Queensland, Queensland 4072, Australia

## Abstract

Forced ignition in an undersped shape-transitioning scramjet engine is numerically investigated, focusing on Mach 6 operation of an engine designed for Mach 8 flight. Initially the flowfield is nonreacting, being too cold to ignite, with a large recirculation region behind the fuel injector in the thickest part of the boundary layer. A hot zone resembling a spark was placed in the flow behind the this injector, which was able to ignite the flow on contact with the wall. Sustained combustion was initiated from this one spark, and altered the flowfield of the injector, forcing separation upstream. Fuel enters this region and establishes a dual mode combustion mechanism. Thus a spark, placed closed to or on the wall, and with an appropriate fuelling scheme, can ignite the flow in an undersped engine and force dual mode combustion in an initially cold flowfield.

## Introduction

A scramjet capable of accelerating from Mach 5 to Mach 10 is of interest to supply the propulsion for the second stage of a small satellite launch system [9]. For a fixed geometry inlet operating at the low speed end of such a trajectory, the average temperature entering the combustor is below that required to autoignite hydrogen, thus a forced ignition system is required. At these speeds, it is also advantageous to use dual-mode (mixing subsonic and supersonic) combustion to generate better performance than pure supersonic combustion [13]. The large regions of subsonic flow that characterize dual mode combustion are usually anchored by physical obstructions to the flow or cavities, but these would result in prohibitive losses at the high speed end of the trajectory. Dual mode combustion in an unobstructed flowpath was explored experimentally by Turner [13]. In the present work, this Mach 8 REST (Rectangular to Elliptical Shape Transition) engine of Turner's is simulated well below its design speed, at Mach 6.2, using an unsteady RANS (Reynolds-Averaged Navier-Stokes) simulation approach.

In the past, large-eddy simulation (LES) studies of scramjets in hypersonic flows [3, 4] have been able to simulate spark ignition to replicate experimental results. However, as we want to simulate a practical scramjet engine design we are limited to unsteady RANS (URANS) simulations; as LES are too computationally expensive. To the best of the authors' knowledge, this is the first URANS investigation of spark ignition in a flight candidate scramjet engine without the aid of cavity or ramp flameholders. URANS simulations have been performed in the past to investigate the effects of inlet design on combustor performance and flow structure [7] and to design cavity flameholders for experimental models [2].

## Methodology

To numerically investigate the problem, the flow solver US3D was used, solving the RANS equations in an unsteady manner. US3D was developed at the University of Minnesota [8], and has previously been used to simulate REST style engines in high Mach number scenarios [6]. This simulation was fully turbulent from the leading edge, using the Spalart Allmaras turbulence model [6], and the Jachimowski reaction scheme for hydrogen-air combustion [5].

Separate grids for the inlet and combustor were used to save computational cost, using the flux conserving boundary condition of [6]. Half of the engine was simulated used the symmetry plane down the centre of the engine. A grid convergence study was performed on each using the method of [12], for a simulation not shown in this paper. The fine inlet grid was converged to 0.93%, 1.48%, and 0.93% for stream-wise averaged Mach number, pressure and temperature, when compared to the Richardson extrapolated exact values. For the combustor, the combustion and mixing efficiencies on the fine grid were converged to 1.32% and 1.30% when compared to the extrapolated infinite grid solution. The fine grid solution is presented in this paper. The inlet grid contained 30 million cells, and the combustor grid, 37 million cells.

This simulation has been overfuelled with hydrogen at an equivalence ratio of 1.82, as large equivalence ratios can transition this engine to operate in a dual mode manner at its design point. The spark has dimensions based on those in the experiment of [1], with a temperature of 4600 K, and an elliptical shape of length and width of 0.54 mm, 0.21 mm.

To capture the unsteady effects, a low Courant-Freidrichs-Lewy (CFL) number was used to ensure time accuracy in the cells desired; the region behind the injector where the spark is occurring. Figure 1 shows the maximum timestep for explicit time accuracy, for each cell. A timestep of 75 ns was used in the simulation. In the expansion regions of the fuel injectors, the required time step is below that of the global time step, but has very low unsteadiness.

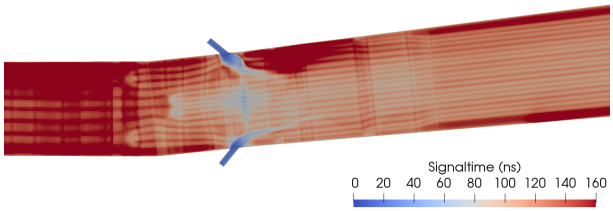


Figure 1: Signal speed time shown based on CFL criteria. This can be used to set a timestep which can capture unsteadiness in the base flow of a RANS simulation

The engine used for the simulation is shown in figure 2. The engine is designed using a streamtracing technique [11]. Bodyside refers to the top of the engine where it attaches to the underside of a hypersonic vehicle, and cowlside refers to the underneath. The ring of 8 porthole injectors used in this engine are shown in figure 3. These are inclined at 45 degrees to the flow.

## Preignition Flowfield

The symmetry plane flowfield in the region near the injectors is shown in figure 4, using contours of temperature, fuel mass fraction, axial velocity and Mach number. No combustion is

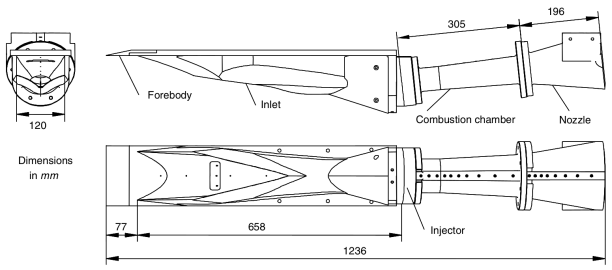


Figure 2: Mach 8 REST Schematic. Reproduced from Turner [13]

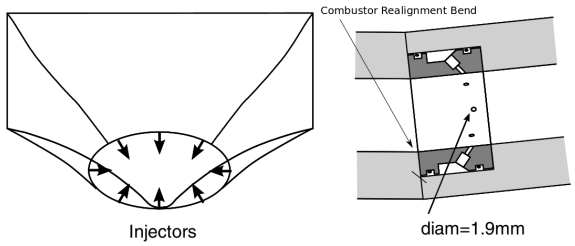


Figure 3: Injector Ring. Reproduced from Turner [13]

occurring in this flow, despite the high equivalence ratio. The temperature is the limiting factor - although it is above the autoignition point of the hydrogen fuel, no region has both a sufficient temperature and access to the fuel.

The region behind the bodyside injector has a large recirculating subsonic zone, which is caused by the impinging of the combined shocks originating from the cowlside injector and the 6 degree combustor realignment bend. This is a region of high local temperature, and has the potential to be a flameholding region if combustion can be forced.

### Spark Flowfield

The symmetry plane region close to the spark location and injectors is shown in figure 5. The spark itself is located in a region on the edge of the fuel plume on the bodyside of the combustor, which can be seen in the temperature plot of figure 5a.

The spark is initially unable to sustain combustion of the flow, due to adverse conditions; equivalence ratio and temperature. A small amount of OH is generated as the spark's effect moves away from its initial location as shown in figures 5b and 5c, but no significant combustion occurs. Note that the OH contour in figure 5c has changed scale so it can still be visualised, as it drops two orders of magnitude. When the spark remnant interacts with the bodyside wall, the favourable conditions generated cause OH radicals to be formed, indicating combustion is initiated, which is seen in figure 5d.

In other simulations, it has been observed that when combustion reaches the rear of the bodyside injector, the interaction between combustion and the injector flowfield forces combustion, and separation, to occur upstream, leading to dual mode combustion. This is the phenomenon we are attempting to force.

As the effects are weakened by the distance to the wall from the initial spark location, we suggest that a spark at the wall would have equal or better performance. In a practical sense, it is easier to place a spark plug or such device at the wall, rather than having an ignition mechanism designed to interact with the central flow.

| Forebody Conditions | |
|---|---|
| Property | Value |
| Mach number | 5.335 |
| Pressure | 4353 Pa |
| Stagnation Pressure | 3.3765 MPa |
| Density | 0.05224 kg/m$^3$ |
| Temperature | 209.3 K |
| Equivalence Ratio | 1.83 |
| Velocity | 1821.97 m/s |

Table 1: Inflow conditions equivalent to a Mach 6.2 freestream

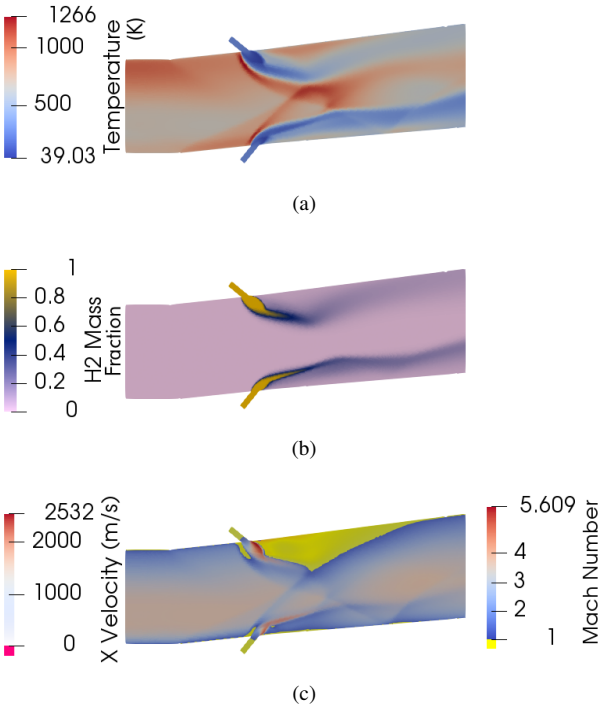


Figure 4: Symmetry plane contour of Temperature, H2 Mass Fraction and Velocity and Mach Number Contours. This flowfield in not combusting due to the low temperatures in the regions where fuel is located.

### Post Ignition Flowfield

The recirculating flowfield has a high fuel content, and once the spark has ignited the flow near the wall, the rest of the recirculating region can begin to combust. Figure 5e shows the consumption of this fuel, which heats and expands the region. The expansion of the wake causes the fuel jet to become steeper and penetrate further, strengthening its bow shock, as can be seen by the changing fuel mass fraction locations in figure 5d, 5e and 5f. Burning now occurs in the shear layer, in figure 5f. The separation size upstream of the injector increases as the fuel jet inclines further to the oncoming flow. Eventually, in figure 5g, fuel can enter this region and combust, which further expands it. Figure 5h shows the final transition to dual mode combustion has occurred with significant combustion occurring upstream of the injector, and large separations in the engine.

### Upstream Propagation

In this simulation, with such extreme overfuelling, the upstream propagation is not balanced and the combustion reaches the start of the combustor grid. The development of the flow is shown in figure 6. Combustion ahead of the bodyside injector moves the separation upstream. The interaction between this separation

and the incoming flow separates the cowlside boundary layer, and combustion occurs in this region as fuel moves ahead of the jet, which is shown in figures 6b and 6c. The combustion occurring ahead of the cowlside jet creates a shock which interacts with the large bodyside separation increasing its size and the combustion within. These interactions are not balanced, and drive the separations upstream.

### Conclusion

We attempted to simulate an undersped scramjet engine, to see whether dual mode combustion could be established in a cold flowfield. Initially, combustion did not occur due to the limiting temperature of the flow. A spark ignition was simulated in an unsteady RANS simulation which showed the ignition model could instigate dual mode combustion. Combustion was sustained but due to the overfuelling, it propagated to the start of the grid.

The spark model showed best performance when its effects reached the wall, which indicated the wall is a more suitable place for a spark ignition system in the engine considered. This present simulation showed the capability to model forced ignition in a scramjet engine using RANS equations, and that dual mode flow can be initiated and sustained in a cold Mach 6 flowfield in an engine designed for Mach 8 flow. This methodology can be used in the design of an engine to be used along an accelerating trajectory.

### Acknowledgements

The authors would like to acknowledge and thank Professor Graham Candler's research group for use of their research CFD code, US3D, as well as the (National Computational Infrastructure) NCI Merit allocation scheme for the computational resources used. This work was supported by resources provided by The Pawsey Supercomputing Centre with funding from the Australian Government and the Government of Western Australia. The first author would like to acknowledge support through the Australian Government Research Training Program.

### References

[1] Brieschenk, S., Pontalier, Q., Duffaut, A., Denman, Z. J., Veeraragavan, A., Wheatley, V. and Smart, M. Characterization of a spark ignition system for flameholding cavities *45th AIAA Plasmadynamics and Lasers Conference*, 2014, 2242

[2] Denman, Z. J.; Brieschenk, S.; Veeraragavan, A.; Wheatley, V. and Smart, M. Experimental Design of a Cavity Flameholder in a Mach 8 Shape-Transitioning Scramjet *19th AIAA International Space Planes and Hypersonic Systems and Technologies Conference*, 2014, 2953

[3] Gibbons, N. N., Gehre, R., Brieschenk, S. and Wheatley, V. Simulation of Laser-Induced-Plasma Ignition in a Hypersonic Crossflow *20th AIAA International Space Planes and Hypersonic Systems and Technologies Conference*, 2015, 3622

[4] Gibbons, N., Gehre, R., Brieschenk, S. and Wheatley, V. Blast Wave-Induced Mixing in a Laser Ignited Hypersonic Flow *Journal of Fluids Engineering, American Society of Mechanical Engineers*, 2018, 140, 050902

[5] Jachimowski, C. J. An analysis of combustion studies in shock expansion tunnels and reflected shock tunnels 1992

[6] Landsberg, W. O.; Gibbons, N. N.; Wheatley, V.; Smart, M. K. and Veeraragavan, A. Improving scramjet performance through flow field manipulation *Journal of Propulsion and Power*, American Institute of Aeronautics and Astronautics, 2017, 34, 578-590

[7] Malo-Molina, F. J.; Gaitonde, D. V.; Ebrahimi, H. B. and Ruffin, S. M. Three-dimensional analysis of a supersonic combustor coupled to innovative inward-turning inlets *AIAA journal*, 2010, 48, 572-582

[8] Nompelis, I.; Drayna, T. and Candler, G. Development of a hybrid unstructured implicit solver for the simulation of reacting flows over complex geometries *34th AIAA Fluid Dynamics Conference and Exhibit*, 2004, 222

[9] Preller, D.; Smart, M. K. and Schutte, A. Dedicated Launch of Small Satellites using Scramjets *AIAA SPACE* 2016, 2016, 5480

[10] Spalart, P. and Allmaras, S. A one-equation turbulence model for aerodynamic flows *30th aerospace sciences meeting and exhibit*, 1992, 439

[11] Smart, M. Design of three-dimensional hypersonic inlets with rectangular-to-elliptical shape transition *Journal of Propulsion and Power*, 1999, 15, 408-416

[12] Stern, F.; Wilson, R. V.; Coleman, H. W. and Paterson, E. G. Comprehensive approach to verification and validation of CFD simulationspart 1: methodology and procedures *Journal of fluids engineering, American Society of Mechanical Engineers*, 2001, 123, 793-802

[13] Turner, J. C. and Smart, M. K. Mode change characteristics of a three-dimensional scramjet at Mach 8 *Journal of Propulsion and Power, American Institute of Aeronautics and Astronautics*, 2013, 29, 982-990

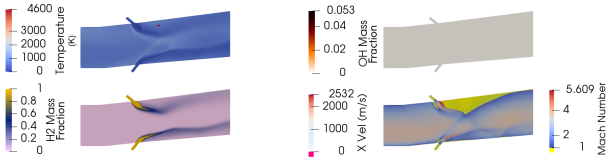


(a) Time = 0.0 ms

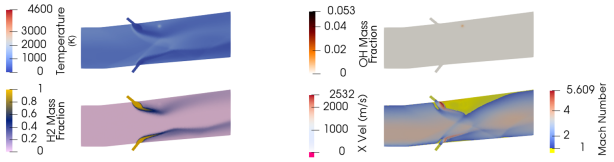


(b) Time = 0.018 ms

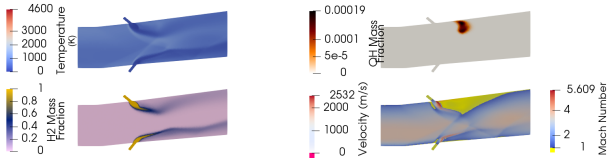


(c) Time = 0.194 ms

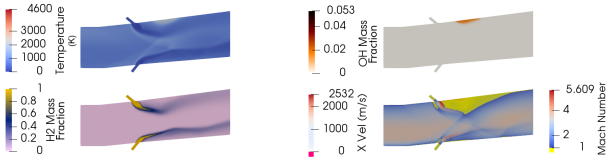


(d) Time = 1.30 ms

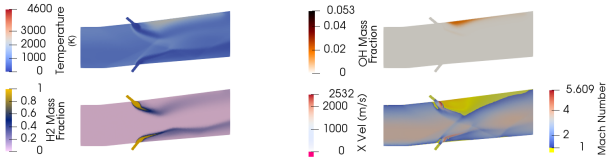


(e) Time = 1.43 ms

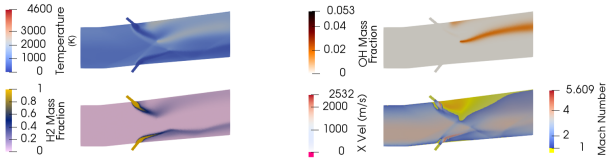


(f) Time = 1.61 ms

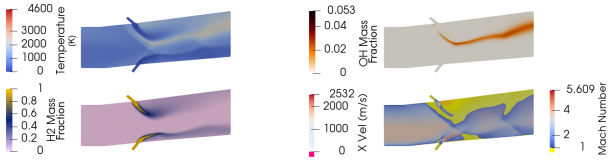


(g) Time = 1.79 ms

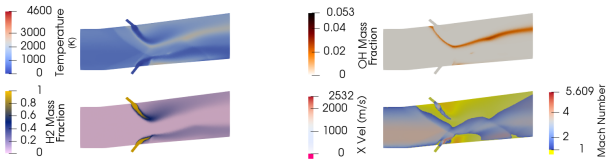


(h) Time = 1.96 ms

Figure 5: Ignition Flowfield with Temperature, OH and H2 Mass Fractions, and Axial Velocity and Mach Number Contours. Sustained combustion occurs when the spark's wave interacts with the wall. Due to the expansion caused by combustion the fuel jet is forced upstream causing greater separation of the boundary layer and increased burning in the shear layer. This allows combustion to occur in the upstream separated boundary layer.

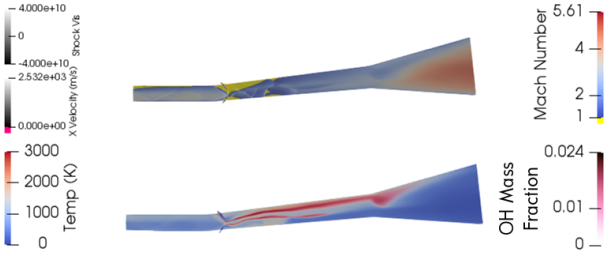


(a) Time = 2.17 ms

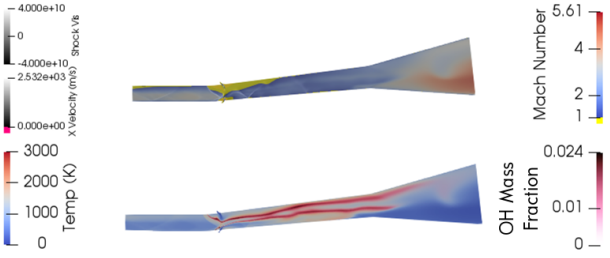


(b) Time = 2.42 ms

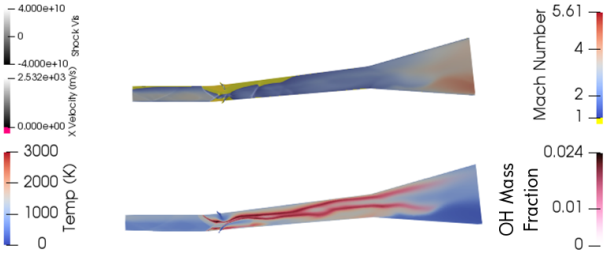


(c) Time = 2.67 ms

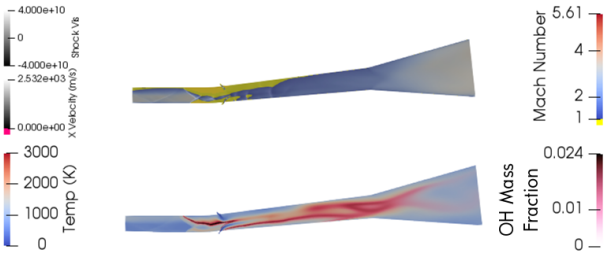


(d) Time = 3.37 ms

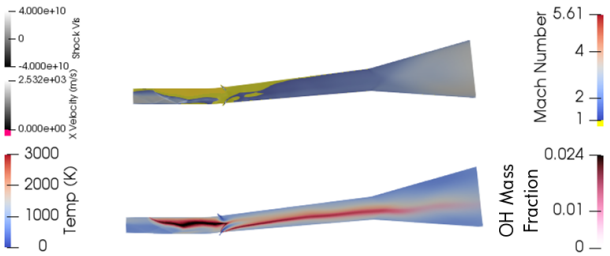


(e) Time = 4.43 ms

Figure 6: Evolution of Spark Ignition Flowfield